MAGNETIC FIELDS IN THE EARLY UNIVERSE[a]

KARI ENQVIST
Department of Physics, P.O. Box 9, FIN-00014 University of Helsinki, Finland

The observed galactic magnetic fields may have a primordial origin. I briefly review the observations, their interpretation in terms of the dynamo theory, and the current limits on cosmological magnetic fields. Several possible mechanisms for generating a primordial magnetic field are then discussed. Turbulence and the evolution of the microscopic fields to macroscopic fields is described in terms of a shell model, which provides an approximation to the full magnetohydrodynamics and indicates the existence of an inverse cascade of magnetic energy. Cosmological seed fields roughly of the order of 10^{-20} G at the scale of protogalaxy, as required by the dynamo explanation of galactic magnetic fields, seem rather plausible.

1 Introduction

Apart from the baryon number and the spectrum of energy density fluctuations, the physical processes that took place in the very early universe do not have many consequences that could still be directly detectable today. Most observables have been washed away by the thermal bath of the pre-recombination era. One possibility, which has recently received increased attention, is offered by the large-scale magnetic fields observed in a number of galaxies, in galaxy halos, and in clusters of galaxies [1]. The astrophysical mechanism responsible for the origin of the galactic magnetic fields is not understood. Instead one postulates a small seed field, which can then be either enhanced by the compression of the protogalaxy, or exponentially amplified by the turbulent fluid motion as in the dynamo theory [2]. The exciting possibility is that the seed field could be truly primordial, in which case cosmic magnetic fields could provide direct information about the very early universe.

The problem then is twofold. First, one has to find a mechanism in the early universe which is able to produce a magnetic field large enough to act as the seed field. There are various proposals, a number of which are based on the early cosmological phase transitions, which are discussed in Sect 3. The second problem is to explain how the initial field, which is expected to be random as it is created by microphysics and having correlation lengths typical to microphysics, can grow up to be coherent enought at large length scales. This is a problem in magnetohydrodynamics which is discussed in Sect 4.

[a]Invited Talk at the Strong and Electroweak Matter '97 21-25 May 1997, Eger, Hungary

2 Observations and limits

2.1 Observing cosmic magnetic fields

Magnetic fields at the level of few μG have been detected in galaxies, in galactic halos, and in clusters of galaxies. They can be observed indirectly at optical and radio wavelengths [1]. The Zeeman splitting of the spectral lines would provide a direct measure of the strength of the magnetic field, but the shifts are very small and this method is applicable mainly to our own galaxy.

Electrons moving in a magnetic field emit synchrotron radiation, and both its intensity and polarization can be used to extract information about the magnetic field. However, one needs first to fix the relative magnitudes of the electron and magnetic field densities. Usually equipartition of magnetic and plasma energies is assumed.

Information about distant magnetic fields in e.g. clusters in galaxies has been obtained by studying the Faraday rotation of polarized light. The method is based on the fact that the plane of polarization of linearly polarized electromagnetic wave rotates as it passes through plasma supporting a magnetic field. The rotation angle $\Delta\chi$ depends on the strength and extension of the magnetic field, the density of plasma, and on the wavelength λ of radiation. The Faraday rotation measure (RM) is defined as

$$\frac{\Delta\chi}{\Delta\lambda^2} = 8.1 \times 10^5 \int n_e B_l dl \text{ rad m}^{-2} , \quad (1)$$

where B_l is the strength of the magnetic field along the line of sight. This method requires some independent information about the electron density and the field reversal scale.

2.2 $\alpha - \omega$ dynamo

The currently favoured explanation for the origin of the large scale galactic magnetic fields is the $\alpha - \omega$ dynamo [2], which through turbulence and differential rotation amplifies a small frozen-in seed field $\mathbf{B}_0$ to the observed μG field. An initially toroidal seed field, which is carried along on the disc of a rotating (spiral) galaxy, is locally distorted into a loop by the up- or downward stochastic drift of the gas. As the gas moves away from the plane of the disc, the pressure decreases and the gas expands; at the same time it is subject to a Coriolis force which will rotate it. The magnetic field lines, glued to the gas, will follow and thus a poloidal component perpendicular to $\mathbf{B}_0$ is generated. The small poloidal loops will reconnect and coalesce to produce a large scale field. This is the so-called α-effect. Because the disc does not rotate like a

rigid body, the field lines will be wrapped and the poloidal field will induce a toroidal field; this is the ω-effect. Thus the dynamo mechanism does not only produce a large scale field but can also, to some extent, predict the shape of the field. In practise one does not attempt to describe the small scale turbulence directly but rather resorts to a mean-field dynamo, where the average induced current is given by $\mathbf{j}_{ind} = \sigma\alpha\mathbf{B}_0$, where σ is conductivity and α is a parameter related to the average drift velocity.

The dynamo saturates when the growth enters the non-linear regime. A typical growth time is of the order of 10^9 years, with the rotation period of the galaxy setting a lower limit on the growth time. Recently it has been argued [3] that the saturation might actually be too fast for a large-scale field to form. The strength of the required initial seed field is rather uncertain, but as a rule of thumb one could use a value like 10^{-20} G on a comoving scale of a protogalaxy (100 kpc).

Another possibility is that the galactic field results directly from a primordial field, which gets compressed when the protogalactic cloud collapses. The primordial field strengths needed are however quite large. In any case, it appears as if a primordial field is required to explain the observed galactic magnetic fields (although it is conceivable that a purely astrophysical solution could exist as well).

2.3 Limits on cosmologial fields

Observing cosmological, intergalactic magnetic fields would be of great importance and would strengthen the case for their truly primordial origin. It has been claimed by Plaga [4] that the arrival times of extragalactic γ-rays could be used to detect fields as weak as 10^{-24} G. The idea is that cosmic rays, originating from far-away objects such as QSOs or gamma-ray bursters, scatter off the background cosmic magnetic field. This gives rise to pair production and a delayed γ-ray which could then be observed, and the ratio of prompt to delayed γ's provides a measure of the strength of the intergalactic magnetic field. The energy spectrum of γ-rays is likewise affected by the intergalactic magnetic field [6]. Ultra-high cosmic ray protons would also be deflected by the intergalactic magnetic fields so that their arrival times could be used [5] to set bounds as low as 10^{-12} G.

A direct limit on cosmological magnetic field has been obtained by considering the rotation measure of a sample of galaxies and quasars, which yields the limit [7] $B \leq 10^{-9}$ G $(\Omega_{\rm IG} h_{100}/0.01)^{-1}$, where Ω_{IG} is the fraction of the ionized gas density of the critical density in the intergalactic medium, and h is the Hubble constant. It has also been suggested that the power spectrum of

the cosmological field could be determined by studying the correlations in the RM for extragalactic sources [8].

If a primordial magnetic field is present at the time of recombination, it will give rise to anisotropic pressures. These would distort the microwave background. Barrow, Ferreira and Silk [9] have recently considered the effect of a magnetic field on the evolution of shear anisotropy in a general anistropic flat universe. They then compared the result with the 4-year COBE data set, and assuming that the whole observed anisotropy is due to magnetic stresses, concluded that if the field can be taken homogeneous, $B \leq 3.4\times10^{-9}$ G $(\Omega_0 h_{50}^2)^{1/2}$. This is a more stringent limit than what can be obtained [10] from primordial nucleosynthesis considerations. These take into account the contribution of the magnetic field to the Hubble expansions rate and to the $n \leftrightarrow p$ reaction rates, plus the fact that the electron wave functions get modified (the phase space of the lowest Landau level is enhanced). The limit thus obtained is $B \leq 10^{11}$ G for a constant B at $T = 10^9$ K, and if the field is inhomogeneous, the limit is less stringent by an order of magnitude.

The anisotropy limit also indicates that the distortions of the Doppler peaks of the microwave background [11] due to a homogeneous magnetic field are unobservable. The Faraday rotation in the polarization of the microwave background could still be observable [12].

3 Generating primordial magnetic fields

There are a number of proposals for the origin of magnetic fields in the early universe, many of them involving the early phase transitions. Fluctuations in the electromagnetic field in a relativistic plasma are by themselves sufficient for generating a small scale random magnetic field [13]. To obtain a seed field for galactic magnetic fields, one however needs fields with much larger coherence lengths.

3.1 Spontaneous charge separation

Magnetic fields may arise in a electrically neutral plasma if local charge separation happens to take place, thus creating a local current. It has been proposed that this could occur during a first order QCD [14] or EW [15,16] phase transition, which proceed by nucleating bubbles of the new phase in the background of the old phase. There one finds net baryon number gradients at the phase boundaries, providing the basis for charge separation, and the seed fields arise through instabilities in the fluid flow. For that one has to require that the growing modes are not damped. Turbulent flow near the walls of the bubbles is then expected to amplify and freeze the transient seed field. The various

hydrodynamical features have been studied in linear perturbation theory by Sigl, Olinto and Jedamzik [16], who argued that on a 10 Mpc comoving scale, field strengths of the order of 10^{-29} G for EW and 10^{-20} G for QCD could be obtained. These might further be enhanced by several orders of magnitude by hydromagnetic turbulence [17,18], which will be discussed in Section 4.3.

3.2 Bubble collisions

In a first order phase transition the phases of the complex order parameter $\Phi = \rho e^{i\Theta}/\sqrt{2}$ of the nucleated bubbles are uncorrelated. When the bubbles collide, there arises a phase gradient which acts as a source for gauge fields. The phase itself is not a gauge invariant concept, but it has been pointed out by Kibble and Vilenkin [19] that a gauge invariant phase difference can be defined in terms of an integral over the gradient $D_\mu\Theta$.

Magnetic field generation in the collision of phase transition bubbles has been considered in the abelian Higgs model [19,20]. One assumes that inside the bubble the radial mode ρ settles rapidly to its equilibrium value η and can thus be treated as a constant. The dynamical variables are thus Θ and the gauge field A^μ. The starting point is the U(1)-symmetric lagrangian

$$\mathcal{L} = -\frac{1}{4}F_{\mu\nu}F^{\mu\nu} + D_\mu\Phi(D^\mu\Phi)^\dagger + V(|\Phi|), \tag{2}$$

where the potential V is assumed to have minima at $\rho = 0$ and $\rho = \eta$. The simplest case is that two spherical bubbles nucleate, one at $(x, y, z, t) = (0, 0, z_0, 0)$ and the other at $(x, y, z, t) = (0, 0, -z_0, t_0)$, and keep expanding with the velocity v even after colliding. Because of the symmetry of the problem, the solutions to the equations of motion are functions of z and $\tau = \sqrt{t^2 - x^2 - y^2}$ only, and the U(1) gauge field $A^\mu = x^\mu f(\tau, z)$. With the appropriate initial conditions, the solutions are [19]

$$\begin{aligned}
\Theta &= \frac{\Theta_0 R}{\pi\tau}\int_{-\infty}^{\infty}\frac{dk}{k}\sin k(z-z_1)\big[\cos\omega(\tau-R) + \frac{1}{\omega R}\sin\omega(\tau-R)\big]\ , \\
f &= \frac{\Theta_0 R e\eta^2}{\pi\tau^3}\int_{-\infty}^{\infty}\frac{dk}{k}\sin k(z-z_1)\big[\frac{R-\tau}{\omega^2 R}\cos\omega(\tau-R) \\
&+ \big(\frac{\tau}{\omega} + \frac{1}{\omega^3 R}\big)\sin\omega(\tau-R)\big],
\end{aligned} \tag{3}$$

where $\omega \equiv \sqrt{k^2 + e^2\eta^2}$, R is the radius of the bubbles at the collision and z_1 the point of first collision on the z-axis. Here the velocity of the bubbles has been taken to be $v = 1$. The generated magnetic field is rapidly oscillating and orthogonal to the z-axis and in this case confined inside the intersection

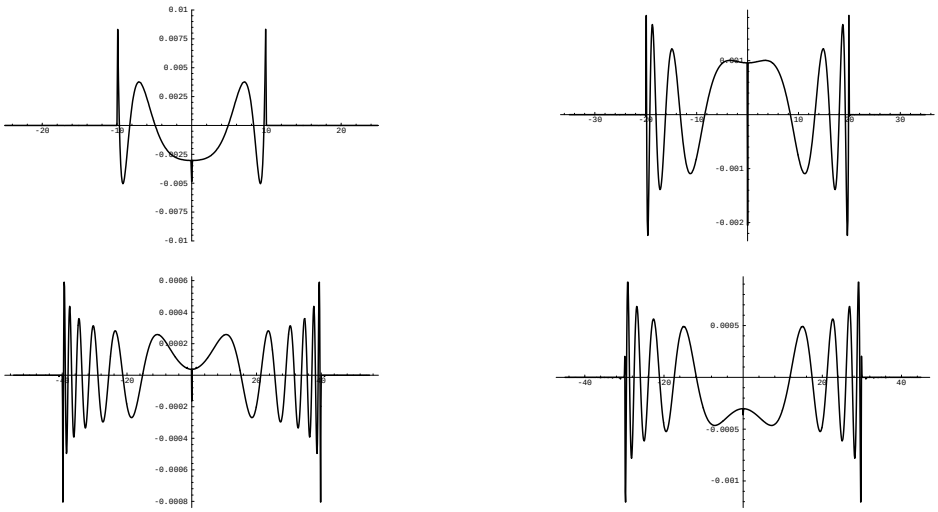

Figure 1: The time evolution of B along the radius $r = 1$ for t=10, 20, 30 and 40 after the initial collision. The radius of the bubbles at the collision has been chosen here $R = 10$, and the collision point on the z-axis is $z_1 = 50$. (The units are such that $e\eta = 1$).

region, as can be seen from Fig. 1. It has a ring-like shape in the (x,y)-plane. It can be shown that subsequent collisions of the bubbles, which now may have a magnetic field inside the bubbles, nevertheless lead to a qualitatively similar outcome [20].

There are however two additional important ingredients which need to be taken into account: the high but finite conductivity [21,22] of the primordial plasma and the fact that in the electroweak phase transition the bubbles will in fact intersect with non-relativistic velocities [23]. Finite conductivity gives rise to diffusion, the consequence of which is to smooth out the rapid oscillations of $\mathbf{B}$, whereas low v will permit the magnetic flux to escape the intersection region and penetrate the colliding bubbles, where its evolution will be governed by usual magnetohydrodynamics. The resulting behaviour is demonstrated in Fig 2.

The strength of the generated magnetic field depends on the bubble wall velocity in an essential way [20]. In the electroweak case the initial growth of the bubble wall is by subsonic deflagration, with velocities of the order of $0.05c$, depending on the assumed friction strength [23]. The wall is preceded by a shock front, which may collide with the other bubbles. This results in reheating, and

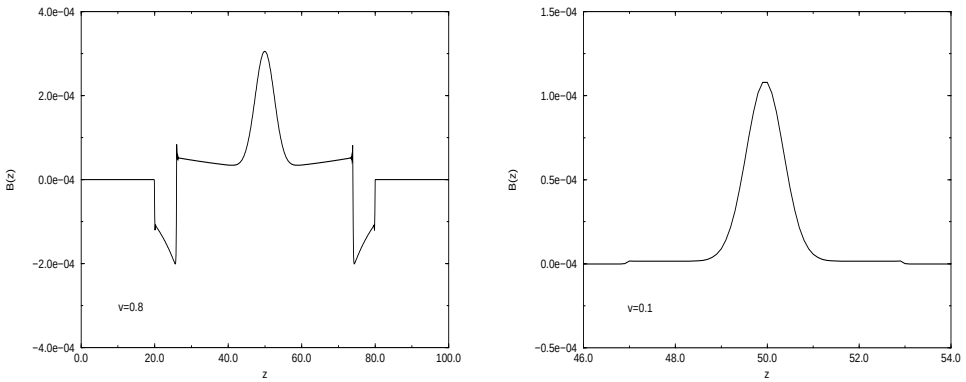

Figure 2: B along $r = 1$ with $R = 10$ at $t = 30$ after collision with $v = 0.8$ and 0.1. Here conductivity has been taken to be $\sigma = 7T$ The point of initial collision on the z-axis is $z_1 = 50$, and the outer edge of the intersection region is at $\simeq 50 \pm vt$. The outer edge of the magnetic field is at $\simeq 50 \pm t$ (and units are $e\eta = 1$).

oscillations of the bubble radii, but eventually a phase equilibrium is attained. The ensuing bubble growth is very slow and takes place because of the expansion of the universe. Because the universe has been reheated back to T_c, no new bubbles are formed during the slow growth phase. Assuming that the abelian Higgs model results are applicable to the electroweak case, as seems to be the case [24], one may estimate that [20]

$$B \simeq 2.0 \times 10^{20} \sqrt{\gamma^2 + 2\gamma R}/R \ \text{G}, \tag{4}$$

where it has been assumed $\Theta_0 = 1$, $T_c = e\eta = 100$ GeV; the average distance between the nucleation centers $r_{ave} = 9.5 \times 10^{-8} t_H$ and the velocity $v = 1.2 \times 10^{-4}$ were taken as reference values. Folding in the spectrum of separation of the adjacent shocked spherical bubbles [25], averaging over all possible inclinations of the ring-like magnetic field, and taking into account the enhancement of magnetic energy due to an inverse cascade (see next Section), one arrives at the estimate $B_{rms} \simeq 10^{-21}$G for the cosmological magnetic field at the scale of 10 Mpc today [20].

3.3 Fluctuating Higgs gradients

It has been pointed out by Vachaspati [26] that fluctuating Higgs field gradients will induce a magnetic field. Such local fluctuations are naturally present at the EW phase transition, since the embedding of the electromagnetic field in

$SU(2) \otimes U(1)_Y$ involves these gradients:

$$\begin{aligned} F_{ij}^{em} &= -i(V_i^\dagger V_j - V_i V_j^\dagger) \ , \\ V_i &= \frac{2}{|\phi|}\sqrt{\frac{\sin\theta}{g}}\,\partial_i\phi \ , \end{aligned} \tag{5}$$

where ϕ is the Higgs field. (An argument against horizon-size fluctuations has been presented by Davidson [27]). At the electroweak phase transition the correlation length in the broken phase is $\sim 1/m_W$ (assuming that the Higgs mass is comparable to m_W). The field strength F_{ij}^{em} is thus constant over a distance $\sim 1/m_W$, but it varies in a random way over larger distances in order to respect causality. The vector V_i is also random, of course. Its variation is due to the fact that the Higgs field ϕ makes a random walk on the vacuum manifold of ϕ. The problem then is to estimate the field strength F_{ij}^{em} over a length scale $\sim N/m_W$. If $N = 1$, then it follows on dimensional grounds that the root-mean-square $F_{ij}^{em} \sim m_W^2 \sim 10^{24}$ G. For N large, one should use a statistical argument. Vachaspati argued that the gradients are of order $1/\sqrt{N}$, since ϕ makes a random walk on the vacuum manifold with $\Delta\phi \sim \sqrt{N}$, and since $\Delta x \sim N$. Thus V_i is, in a root mean square sense, of the order $1/\sqrt{N}$, and hence F_{ij}^{em} is of order $1/N$. Taking further into account that the flux in a co-moving circular contour is constant, the field must decrease like $1/a(t)^2$, where $a(t)$ is the scale factor. However, there also exists a different statistical scenario, based on a line average, where the gradient vectors are taken to be the basic stochastic variables [28]. The field strength can be interpreted statistically in such a way that the mean magnetic field satisfies

$$\langle F_{ij}^{em}\rangle_T = 0 \ , \qquad \sqrt{\langle F_{ij}^2\rangle_T} \sim \frac{T^2}{\sqrt{N}} \ . \tag{6}$$

One observes that the scaling behavior is weaker by a factor $\sqrt{N}$. This means that for a scale of 100 kpc

$$\sqrt{\langle F_{ij}^2\rangle_{today}} \sim 10^{-18}\mathrm{G} \ , \tag{7}$$

which is very close to the value desired for the dynamo effect. Because the Faraday rotation involves the average along the line of sight, this averaging method could indeed be appropriate for those observations.

3.4 Vacuum condensates

Another, more exotic possibility for generating primordial magnetic fields is based on the observation that, due to quantum fluctuations, the Yang–Mills

vacuum is unstable in a large enough background magnetic field [29] at zero temperature. There are indications from lattice calculations that this is a non-perturbative result [30]. In a pure SU(N) theory at the one–loop level the zero temperature effective energy for a constant background non–abelian magnetic field reads [29]

$$V(B) = \frac{1}{2}B^2 + \frac{11N}{96\pi^2}g^2B^2\left(\ln\frac{gB}{\mu^2} - \frac{1}{2}\right) \tag{8}$$

with a minimum at

$$gB_{\rm min} = \mu^2 \exp\left(-\frac{48\pi^2}{11Ng^2}\right) \tag{9}$$

and $V_{\rm min} \equiv V(B_{\rm min}) = -0.029(gB_{\rm min})^2$. Thus the ground state has a non–zero non–abelian magnetic field, the magnitude of which is exponentially suppressed relative to the renormalization scale, or the typical momentum scale of the system. In the early universe, however, where possibly a grand unified symmetry is valid, the exponential suppression may be less severe. It is also attenuated by the running of the coupling constant.

In the early universe the effective energy picks up thermal corrections from the fermion, gauge boson, and Higgs boson loops. The detailed form of the thermal correction depends on the actual model, but one may take the cue from the SU(2) one–loop calculation, where they are obtained by summing the Boltzmann factors $\exp(-\beta E_n)$ for the oscillator modes

$$E_n^2 = p^2 + 2gB(n + \frac{1}{2}) + 2gBS_3 + m^2(T), \tag{10}$$

where $S_3 = \pm 1/2$ (± 1) for fermions (vectors bosons). Eq. (10) includes the thermally induced mass $m(T) \sim gT$, corresponding to a ring summation of the relevant diagrams. Numerically, the effect of the thermal mass turns out to be very important. At high temperature, the leading behaviour is given mainly by the bosonic contributions, and thus one arrives at the estimate [31]

$$\delta V_T^v = \frac{(gB)^2}{8\pi^2}\sum_{l=1}^{\infty}\int_0^{\infty}\frac{dx}{x^3}e^{-K_l^b(x)}\left[x\frac{\cosh(2x)}{\sinh(x)} - 1\right], \tag{11}$$

where $K_l^a(x) = gBl^2/(4xT^2) + m_a^2 x/(gB)$ and numerically $\delta V_T^v \sim 0.02\ (gB)^2$ which serves only to shift the value of B at the vacuum slightly. Thus $B \neq 0$ is the state of the lowest energy even at high temperature.

A local fluctuation will then trigger the creation of the a new vacuum with non-zero non–abelian magnetic field inside a given particle horizon at scales $\mu \simeq T$. The Maxwell magnetic field is then just a projection of the

non-abelian field, the order of magnitude of which is given by Eq. (9). One can then estimate that [31]

$$B(T) = g_{\rm GUT}^{-1}\mu^2 \exp\left(-\frac{48\pi^2}{11Ng^2}\right)\left(\frac{T^2}{\mu^2}\right) \simeq 3\times 10^{42}\left(\frac{a(t_{\rm GUT})}{a(t)}\right)^2 \ {\rm G}, \quad (12)$$

where the reference number is for susy SU(5).

Electroweak magnetic condensates have also recently been considered by Cornwall [32], who has suggested that they would give rise to magnetic fields with a net helicity via the generation of electroweak Chern-Simons number. Joyce and Shaposnikov [33] have argued that a right-handed electron asymmetry, generated at the GUT scale, could give induce a hypercharge magnetic field via a Chern-Simons term. Both suggestions deserve further study.

3.5 Inflation and magnetic fields

The basic problem with inflation with regards to magnetic field generation is that the early universe was a good conductor so that, ignoring turbulence, the magnetic flux $\sim Ba^2$ tends to be conserved, where a is the cosmic scale factor. To avoid this, one needs to break the conformal invariance somehow, as was first suggested by Turner and Widrow [21], who considered couplings to the curvature R such as RF^2 and RA^2, as well as photon-axion couplings. Dilaton coupling of the form $e^{\Phi}F^2$ has also been considered [34], and interesting field strengths can be obtained at the expense of tuning the coupling strength. If a phase transition takes place during the inflationary period, a sufficiently large magnetic field can be created, provided however that the phase transition takes place during the final 5 e-foldings [35].

4 From microscopic to macroscopic

Even assuming that a primordial magnetic field is created at some very early epoch, a number of issues remain to be worked out before one can say anything definite about the role of primordial fields for the origin of galactic magnetic fields. At the earliest times magnetic fields are generated by particle physics processes with length scales typical to particle physics. (It has been shown that such fields are stable against thermal fluctuations [36].) The remaining question is whether it is at all possible for the small scale fluctuations to grow to large scales, and what exactly is the scaling behaviour of $B_{\rm rms}$ or the correlator $\langle B(r+x)B(x)\rangle$. To study these problems one needs to consider the detailed evolution of the magnetic field to account for such issues as to what happens when uncorrelated field regions come into contact with each other

during the course of the expansion of the universe. In general, turbulence is an essential feature of such phenomena. These questions can only be answered by considering magnetohydrodynamics (MHD) in an expanding universe [37].

4.1 MHD in curved space

Let us consider the early universe as consisting of ideal fluid with an equation of state of the form $p = \frac{1}{3}\rho$, where p is pressure and ρ the energy density. Let us further assume that the fluid supports a (random) magnetic field. The energy-momentum tensor is then given by

$$\begin{aligned} T^{\mu\nu} &= (p+\rho)U^\mu U^\nu + p g^{\mu\nu} \\ &+ \frac{1}{4\pi}\left(F^{\mu\sigma}F^{\nu}{}_{\sigma} - \frac{1}{4}g^{\mu\nu}F_{\lambda\sigma}F^{\lambda\sigma}\right), \end{aligned} \tag{13}$$

and U^μ is the four-velocity of the plasma, normalized as $U^\mu U_\mu = -1$, and $F_{\mu\nu} = \partial_\mu A_\nu - \partial_\nu A_\mu$ is the electromagnetic field tensor. Note that, as long as diffusion can be neglected, the presence of the magnetic field does not change the equation of state. The magnetic energy is further assumed to be much smaller than the radiation energy, so that one can assume a flat, isotropic and homogeneous universe with a Robertson-Walker metric. Although the magnetic field generates local bulk motion, this may still be consistent with isotropy and homogeneity at sufficiently large scales, in particular if the magnetic field is random, i.e. statistically homogeneous and isotropic on scales much larger than the intrinsic correlation scale of the field.

For numerical treatment it is convenient to write the equations of motion explicitly in 3+1 dimensions and use the conformal time $\tilde{t} \equiv \int dt/a$ as a variable. After a lengthy derivation one arrives at the forms [17]

$$\frac{\partial \tilde{\mathbf{S}}}{\partial \tilde{t}} = -(\boldsymbol{\nabla}\cdot\mathbf{v})\tilde{\mathbf{S}} - (\mathbf{v}\cdot\boldsymbol{\nabla})\tilde{\mathbf{S}} - \boldsymbol{\nabla}\tilde{p} + \tilde{\mathbf{J}}\times\tilde{\mathbf{B}}. \tag{14}$$

and

$$\begin{aligned} \frac{2\gamma^2+1}{4\gamma^2(2\gamma^2-1)}\frac{\partial \ln\tilde{\rho}}{\partial\tilde{t}} &= -\frac{\partial\tilde{\mathbf{S}}^2/\partial\tilde{t}}{\left(\frac{4}{3}\tilde{\rho}\gamma\right)^2(2\gamma^2-1)} \\ &- \mathbf{v}\cdot\boldsymbol{\nabla}\ln(\tilde{\rho}\gamma^2) - \boldsymbol{\nabla}\cdot\mathbf{v} + \frac{\tilde{\mathbf{J}}\cdot\tilde{\mathbf{E}}}{\frac{4}{3}\tilde{\rho}\gamma^2}, \end{aligned} \tag{15}$$

where we have set $\rho + p = \frac{4}{3}\rho$. The Maxwell equations can be written explicitly as

$$\frac{\partial\tilde{\mathbf{B}}}{\partial\tilde{t}} = -\nabla\times\tilde{\mathbf{E}}, \quad \boldsymbol{\nabla}\cdot\tilde{\mathbf{B}} = 0, \tag{16}$$

and

$$\tilde{\mathbf{J}} = \boldsymbol{\nabla} \times \tilde{\mathbf{B}} - \frac{\partial \tilde{\mathbf{E}}}{\partial \tilde{t}}, \quad \boldsymbol{\nabla} \cdot \tilde{\mathbf{E}} = \tilde{\rho}_e \tag{17}$$

where ρ_e is the charge density and $\tilde{\rho}_e = a^3 \rho_e$. Further,

$$\tilde{\mathbf{E}} = -\mathbf{v} \times \tilde{\mathbf{B}}, \tag{18}$$

which is valid in the limit of high conductivity.

The evolution of a random magnetic field configuration in 2d is shown in Fig. 3 for a lower and higher resolution. As time goes on, the coalescence of magnetic structures is seen to lead to the gradual formation of larger and larger scales. Such a behaviour is encouraging, indicating that the field is not really comovingly frozen. On the other hand, 2d MHD is very different from the 3d MHD, and moreover, the Reynolds number in the simulation (about 10) is wildly unrealistic. However, Dimopoulos and Davis [38] have also pointed out that when two initially uncorrelated domains come into contact, the field at the interface should untangle with the plasma bulk velocity v to avoid the creation of domain walls. They propose that the correlation length ξ evolves according to

$$\frac{d\xi}{dt} = H\xi + v \ , \tag{19}$$

where H is the Hubble parameter and the velocity v depends dynamically on B and should, in principle, be determined from MHD. Nevertheless, (19) again points towards the possibility of the magnetic field not necessarily being comovingly frozen.

4.2 Shell models

In ordinary hydrodynamics many properties of turbulence, in particular those related to energy transfer and to the spectral properties have been studied successfully using a simple cascade model. This is true not only qualitatively, but also quantitatively, which is the reason why the cascade model is now much used in studies of nonlinear physics [39].

The basic idea is that the interactions due to the nonlinear terms in the MHD equations are local in wavenumber space, and in k-space the quadratic nonlinear terms become a convolution. Interactions in k-space involving triangles with similar side lengths have the largest contribution. This has led to the shell model which is formulated in the space of the modulus of the wave numbers. This space is approximated by N shells, where each shell consists of wave numbers with $2^n \leq k \leq 2^{n+1}$ (in the appropriate units). The Fourier transform of the velocity over a length scale k_n^{-1} ($k_n = 2^n$) is given by the

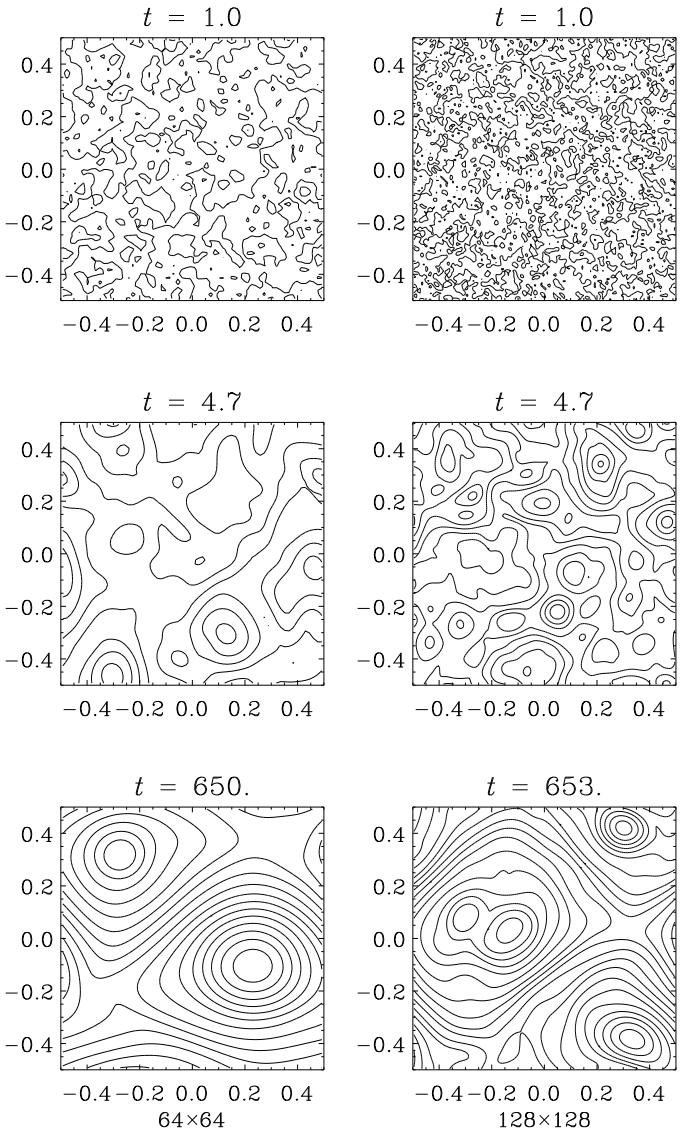

Figure 3: Left column: magnetic field lines at different times at low resolution (64×64 meshpoints). Right column: magnetic field lines at different times at higher resolution (128×128 meshpoints).

complex quantity v_n, and B_n denotes a similar quantity for the B-field. Furthermore, the convolution is approximated by a sum over the nearest and the next nearest neighbours,

$$N_n(v,B) = \sum_{i,j=-2}^{2} C_{ij} v_{n+i} B_{n+j}. \tag{20}$$

Here v and B have lost their vectorial character, which reflects the fact that this model is not supposed to be an approximation of the original equations, but should be considered as a toy model that has similar *conservation* properties as the original equations.

Velocity and magnetic fields are thus represented by scalars at the discrete wave numbers $k_n = 2^n$ $(n = 1, ..., N)$, i.e. k_n increases exponentially. Therefore such a model can cover a large range of length scales (typically up to ten orders of magnitude). The important conserved quantity is $E_{\rm tot} R^4$, where $E_{\rm tot} = \int T^{00} d^3x$ is the total energy. The resulting equations of motion read [17]

$$\tfrac{4}{3}\rho_0 \frac{dv_n}{d\tilde{t}} = N_n(v,b), \tag{21}$$

$$\frac{db_n}{d\tilde{t}} = M_n(v,b), \tag{22}$$

where

$$\begin{aligned} 2N_n(v,b) \quad &= ik_n(A+C)(v^*_{n+1}v^*_{n+2} - b^*_{n+1}b^*_{n+2}) \\ &+ik_n(B-\tfrac{1}{2}C)(v^*_{n-1}v^*_{n+1} - b^*_{n-1}b^*_{n+1}) \\ &-ik_n(\tfrac{1}{2}B+\tfrac{1}{4}A)(v^*_{n-2}v^*_{n-1} - b^*_{n-2}b^*_{n-1}), \end{aligned} \tag{23}$$

$$\begin{aligned} M_n(v,b) \quad &= ik_n(A-C)(v^*_{n+1}b^*_{n+2} - b^*_{n+1}v^*_{n+2}) \\ &+ik_n(B+\tfrac{1}{2}C)(v^*_{n-1}b^*_{n+1} - b^*_{n-1}v^*_{n+1}) \\ &-ik_n(\tfrac{1}{2}B-\tfrac{1}{4}A)(v^*_{n-2}b^*_{n-1} - b^*_{n-2}v^*_{n-1}), \end{aligned} \tag{24}$$

with A, B, and C being free parameters. It is straightforward to verify that $2\sum v^*_n N_n + \sum b^*_n M_n = 0$, using that $k_n = 2^n$.

4.3 Inverse cascade

The numerical study of the cascade model requires of course that the parameters A, B, C are fixed so that the model has the same conservation laws as the full-fledged MHD. The model can then be solved numerically [17], and the results are shown in Fig. 4, where the transfer of magnetic energy to larger and larger length scales is clearly seen. This process, the inverse cascade, is due to the nonlinear terms giving rise to mode interactions. The initial magnetic

energy spectrum was chosen to be given by $E_M(t=0) \sim k$ with the total magnetic energy equal to ρ_0. The number of shells was $N = 30$ so that length scales differing by ten orders of magnitude were covered. It was found that the integral scale, which measures where most magnetic energy is concentrated and which is given by

$$l_0 = \int (2\pi/k) E_M(k) dk \Big/ \int E_M(k) dk, \tag{25}$$

where $E_M(k)$ is the magnetic energy spectrum, increases with the Hubble time approximately like $t_H^{0.25}$.

However, around the time of recombination the photon mean free path λ_γ became very large and photon diffusion became very efficient in smoothing out virtually all inhomogeneities of the photon-baryon plasma [40]. This process is often referred to as Silk damping, which corresponds to a kinematic viscosity $\nu \simeq \lambda_\gamma$ (in natural units). Silk damping may thus destroy the magnetic field, as has been noted by Jedamzik, Katalinic and Olinto [41]. Therefore one has to follow numerically the evolution of the magnetic and kinetic energy spectra in the presence of kinematic viscosity. The results [18] are presented in Fig. 5 and the main point can be summarized as follows: in the cascade models magnetic energy is transferred to large length scales even in the presence of large viscosity. Here the initial magnetic spectrum was chosen to be flat in accordance with the large time behaviour suggested by Fig. 4.

For a sufficiently large viscosity, the inverse cascade stops. One may estimate [18] that this typically takes place close to recombination. The results suggest that in the real MHD, inverse cascade is operative and is essentially not affected by Silk damping, except very late and perhaps for very weak fields. Thus we may conclude that it is unlikely that an equipartition exists in the very early universe. A similar conclusion can be drawn in a different, continuous model where the inverse cascade can be found analytically in an appropriate scaling regime [18,42].

5 Conclusions

Explaining the galactic magnetic fields in terms of microphysical processes that took place when the universe was only ten billionth of a second old is a daunting task, which is not made easier by the complicated evolution of the magnetic field as it is twisted and tangled by the flow of plasma. It is nevertheless encouraging that mechanisms for generating primordial magnetic fields of suitable size exist, and in particular those based on the early cosmological phase transitions discussed in Sect. 3 look promising. At the same

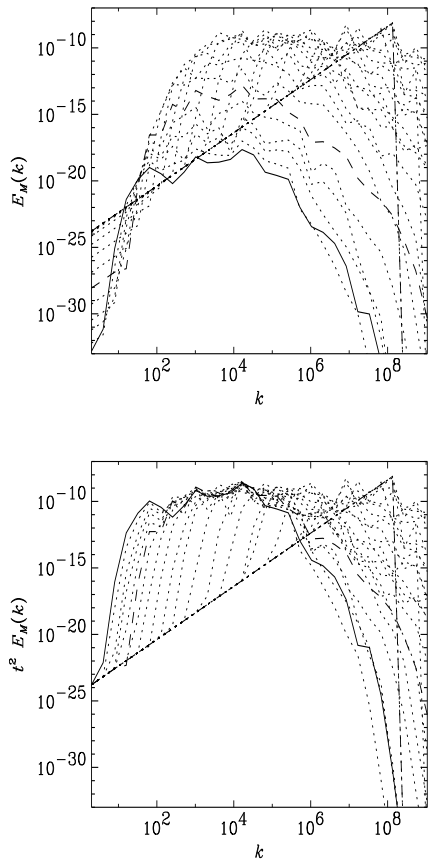

Figure 4: Spectra of the magnetic energy at different times. The straight dotted-dashed line gives the initial condition ($t_0 = 1$), the solid line gives the final time ($t = 3 \times 10^4$), and the dotted curves are for intermediate times (in uniform intervals of $\Delta \log(t - t_0) = 0.6$). $A = 1$, $B = -1/2$, and $C = 0$.

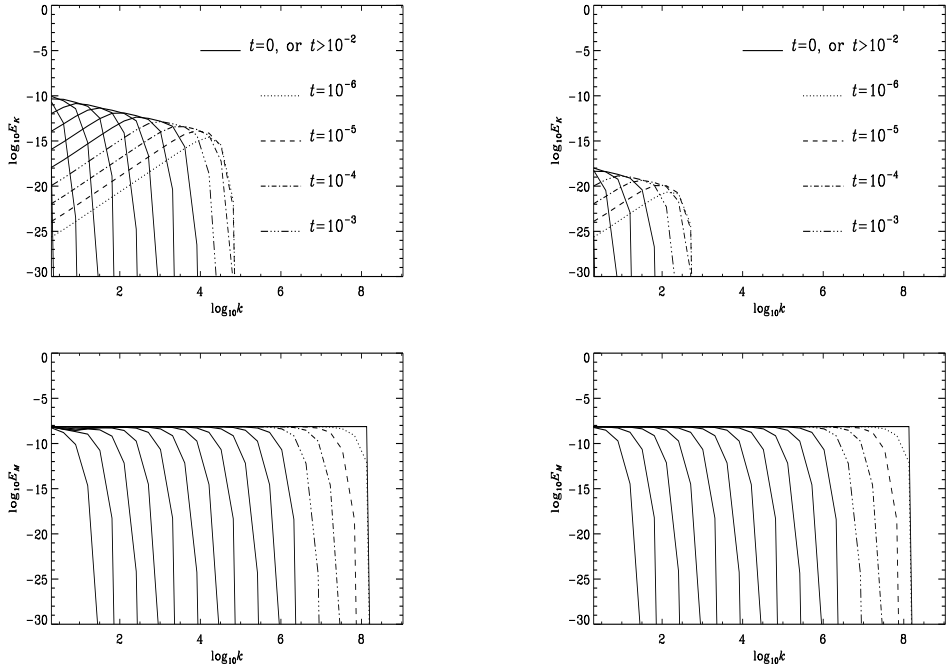

Figure 5: Magnetic and plasma kinetic energy spectrum as a function of the wave number k in the cascade model for small ($\nu = 10^{-2}$) plasma viscosity (left) and large ($\nu = 10^{2}$) plasma viscosity (right). The highest time is $t = 10^{8}$, corresponding to a Hubble time 10^{16}.

time the fact that there are so many possibilities tend to underline our ignorance of the details of the subsequent evolution of the magnetic field. The step from microphysics to macroscopic fields is a difficult one because of the very large magnetic Reynolds number of the early universe. However, different considerations, both analytic approximations, 2d simulations, as well as the full-fledged shell model computations which can account for turbulence, seem to point to the existence of an inverse cascade of magnetic energy. Moreover, as discussed in Sect. 4.3, the inverse cascade is obtained also in the presence of a large plasma viscosity. Therefore the primordial origin of the galactig magnetic fields is quite possible.

Much theoretical work remains to be done, though. At the same time it is very important that progress is made on the observational front. In particular, measuring or setting a stringent limit on the intergalactic field, which could be possible in the near future as indicated in Sect. 2.3, would provide the testing ground for all theoretical scenarios.

References

1. For recent reviews, see P.P. Kronberg, *Rep. Prog. Phys.* **57** (1994) 325; R. Beck et. al., *Ann. Rev. Astron. Astrophys.* **34** (1996) 153.
2. L. D. Landau and E.M. Lifshitz, *Electrodynamics of Continuous Media* (Pergamon, Oxford 1960); Ya.B. Zeldovich, A.A. Ruzmaikin and D.D. Sokoloff, *Magnetic Fields in Astrophysics* (McGraw-Hill, New York, 1980); E.N. Parker, *Cosmological Magnetic Fields* (Oxford Univ. Press, Oxford, 1979); A.A. Ruzmaikin, A.A. Shukurov and D.D. Sokoloff, *Magnetic Fields of Galaxies* (Kluwer, Dordrecht, 1988).
3. S.I.Vainshtein, E. N. Parker and R. Rosner, *Ap. J.* **404** (1993) 773; F. Cattaneo, *Ap. J.* **434** (1994) 200.
4. R. Plaga, *Nature* **374** (1995) 430.
5. M. Lemoine, G. Sigl, A. V. Olinto and D. N. Schramm, astro-ph/9704203.
6. S. Lee, A. V. Olinto and G. Sigl, *Ap. J.* **455** (1995) L21.
7. J.P. Vallée, *Ap. J.* **360** (1990) 1.
8. T. Kolatt, astro-ph/9704243.
9. J.D. Barrow, P. Ferreira and J. Silk, *Phys. Rev. Lett.* **78** (1997) 3610.
10. D. Grasso and H. Rubinstein, *Phys. Lett.* **B379** (1996) 73; B.-l. Cheng A. V. Olinto, D. N. Schramm and J. W. Truran, *Phys. Rev.* **D54** (1996) 4714; P.J. Kernan, G.D. Starkman and T. Vachaspati, *Phys. Rev.* **D54** (1996) 7207.
11. J. Adams, U.H. Danielsson, D. Grasso and H. Rubinstein, *Phys. Lett.* **B388** (1996) 253.

12. A. Kosowsky and A. Loeb, *Ap. J.* **469** (1996) 1.
13. D. Lemoine, *Phys. Rev.* **D51** (1995) 2677.
14. B. Cheng and A.V. Olinto, *Phys. Rev.* **D50** (1994) 2421.
15. G. Baym, D. Bdeker and L. McLerran, *Phys. Rev.* **D53** (1996) 662.
16. G. Sigl, A.V. Olinto and K. Jedamzik, *Phys. Rev.* **D55** (1997) 4582.
17. A. Brandenburg, K. Enqvist and P. Olesen, *Phys. Rev.* **D54** (1996) 1291.
18. A. Brandenburg, K. Enqvist and P. Olesen, *Phys. Lett.* **B391** (1997) 395.
19. T. W. B. Kibble and A. Vilenkin, *Phys. Rev.* **D52** (1995) 679.
20. J. T. Ahonen and K. Enqvist, hep-ph/9704334.
21. M.S. Turner and L.M. Widrow, *Phys. Rev.* **D37** (1988) 2743.
22. J.T. Ahonen and K. Enqvist, *Phys. Lett.* **B382** (1996) 40; G. Baym and H. Heiselberg, astro-ph/9704214.
23. For a recent numerical study, see H. Kurki-Suonio and M. Laine, *Phys. Rev. Lett.* **77** (1996) 3951.
24. D. Grasso and A. Riotto, hep-ph/9707265.
25. B.S. Meyr, C.R. Alcock and G.J. Mathews, *Phys. Rev.* **D43** (1991) 1079.
26. T. Vachaspati, *Phys. Lett.* **B265** (1991) 258.
27. S. Davidson, *Phys. Lett.* **B380** (1996) 253.
28. K. Enqvist and P. Olesen, *Phys. Lett.* **B319** (1993) 178.
29. G.K. Savvidy, *Phys. Lett.* **71** (1977) 133.
30. H.D. Trottier and R.M.Woloshyn, *Phys. Rev. Lett.* **70** (93) 2053.
31. K. Enqvist and P. Olesen *Phys. Lett.* **B329** (1994) 195.
32. J.M. Cornwall, hep-th/9704022.
33. M. Joyce and M. Shaposnikov, astro-ph/9703005.
34. B. Ratra, *Ap. J.* **391** (1992) L1.
35. A-C. Davis and K. Dimopoulos *Phys. Rev.* **D55** (1997) 7398.
36. A. P. Martin and A-C. Davis, *Phys. Lett.* **B360** (1995) 71.
37. R. M. Gailis, N. E. Frankel, and C. P. Dettmann, *Phys. Rev.* **D52** (1995) 6901.
38. K. Dimopoulos and A-C. Davis *Phys. Lett.* **B390** (1997) 87.
39. For a review and further references, see T. Bohr, M. H. Jensen, G. Paladin and A. Vulpiani, *Dynamical Systems Approach to Turbulence*, Cambridge Nonlinear Science Series (Cambridge University Press, 1996).
40. J. Silk, *Ap. J.* **151** (1968) 459.
41. K. Jedamzik, V. Katalinic, and A. Olinto, astro-ph/9606080
42. P. Olesen, *Phys. Lett.* **B398** (1997) 321.